Axisymmetric dynamic instability of polar orthotropic sandwich annular plate with ER damping treatment

Jia-Yi Yeh[*]

Department of Information Management, Chung Hwa University of Medical Technology,
89, Wen-Hwa 1st ST. Jen-Te Hsiang, Tainan County 717, Taiwan, R.O.C.

Abstract. The axisymmetric dynamic instability of polar orthotropic sandwich annular plate combined with electrorheological (ER) fluid core layer and constraining layer are studied in this paper. And, the ER core layer and constraining layer are used to improve the stability of the annular plate system. The boundaries of instability regions for the polar orthotropic sandwich annular plate system are obtained by discrete layer annular finite element and the harmonic balance method. The rheological property of an electrorheological material, such as viscosity, plasticity, and elasticity can be controlled by applying different electric field strength. Thus, the damping characteristics of the sandwich system are more effective when the electric field is applied on the sandwich structure. Additionally, variations of the instability regions for the polar orthotropic sandwich annular plate with different applying electric field strength, thickness of ER layer and some designed parameters are investigated and discussed in this study.

Keywords: dynamic instability; polar orthotropic; electrorheological; annular plate; discrete layer annular finite element

1. Introduction

The dynamic instability may occur when the structure is applying periodic loads or under a range of excitation frequency. Thus, the induced violent vibration is called the dynamic instability or parametric resonance. In the recent years, the dynamic behaviors for the mechanical system were received a great deal of attentions. Bolotin (1964) presented a series of studies on the dynamic instability problems due to the periodic in-plane loads.

The investigations for the dynamic instability or parametric resonance problems of the single circular and annular plate due to the periodic loads were studied and discussed by many researchers. Dumir and Shingal (1985) investigated the axisymmetric postbuckling of polar orthotropic thick annular plates. Then, Chen and Hwang (1988) studied the axisymmetric dynamic instability problem of isotropic and polar orthotropic circular plate by employing Galerkin and finite element methods. Lin and Tseng (1998) studied the free vibration problems of polar orthotropic circular and annular plates. The vibration and dynamic instability of the viscoelastic plate was discussed by Ilyasov and Akoz (2000). The dynamic instability problem of the annular

---

∗Corresponding author, Professor, E-mail: yeh@mail.hwai.edu.tw

plate system with constraining damping treatment by using the finite element method was obtained by Chen and Chen (2004). Then, the buckling of simply-supported rectangular Reissner–Mindlin plates subjected to linearly varying in-plane loading was discussed by Zhong and Gu (2006). And, Wang *et al.* (2006) presented the accurate buckling load problems of thin rectangular plates under parabolic edge compressions by the differential quadrature method. The dynamic behaviors of axially moving viscoelastic plate with varying thickness were studied by Zhou and Wang (2009). Pawlus (2011) studied the solution to the problem of axisymmetric and asymmetric dynamic instability of three-layered annular plates. After that, the dynamic instability of composite plates subjected to non-uniform in-plane loads can be obtained and discussed by Ramachandra and Panda (2012).

Recent developments in smart materials and the potential structural applications had resulted in significant improvements in vibration control systems. Electrorheological (ER) fluid is one of the active smart materials and with controllable rheological properties when an electric field is applied to these fluids. The ER fluid deformed within the small strain range was assumed to be a linearly viscoelastic material with field-dependent complex modulus in the work by Lee (1992). Roy and Ganesan (1993) presented the finite element method to calculate the vibration and damping analysis of circular plate with constrained layer treatment. The vibration characteristics of the sandwich beam system with ER fluid core layer and the variations of the modal loss factors with different designed parameters of the sandwich system were calculated and discussed by Yalcintas and Coulter (1995). Then, Don and Coulter (1995) investigated the analytical and experimental results of the ER material based adaptive beam system. Oyadiji (1996) presented that the modal parameters were more dependent on the location and also discussed the effect of the size of the ER fluid treatment for an aluminum plate. The passive and active damping characteristics of the ER composite beams and the flexural vibration of laminated composite ER sandwich beams to maximize the possible damping capacity was calculated and discussed by Kang *et al.* (2001). Phani and Venkatraman (2003) presented the numerical and experimental results of the sandwich beam using ER fluid. After that, the dynamic characteristics and damping effects of the sandwich isotropic and orthotropic circular plate structures were presented by Yeh (2007) and Yeh *et al.* (2009). And, then Yeh (2011) presented the parametric resonance analysis of axisymmetric sandwich annular plate with ER core layer.

The axisymmetric dynamic instability characteristics and effects of damping properties for polar orthotropic sandwich annular plate with an ER fluid core and constraining layer are presented in the study. To the author's knowledge, no prior work has addressed the axisymmetric dynamic instability problem of polar orthotropic sandwich annular plate with ER fluid core layer. The discrete layer annular finite element and the harmonic balance method are utilized to calculate and obtain the instability regions of polar orthotropic sandwich annular plate system. And, the complex problems of the sandwich annular plate system are solved by using the complex modulus representation of the ER fluid. The effects of the ER layer, applying electric field strength and some designed parameters on the instability regions for the sandwich annular plate system are also investigated and discussed in this paper. In this study, the significant effects on the axisymmetric dynamic characteristics of polar orthotropic sandwich annular plate with ER core layer can be seen.

2. Analytical model formulation

In Fig. 1, the polar orthotropic sandwich annular plate with ER core layer and constraining layer subjected to the uniform radial stress is demonstrated. As shown in the figure, layer 1 is a pure elastic, isotropic constraining layer and the ER fluid core layer is designed as layer 2 and the properties of the ER material can be changed and controlled by applying different electric field strength. Layer 3 is the annular plate with an inner radius a and outer radius b and assumed to be elastic, undamped and polar orthotropic. And, the thicknesses of the three layers of the sandwich annular plate system are h_1, h_2, and h_3, respectively. Additionally, the following assumptions should be mentioned in order to simplify present problems. It is assumed that there are no slipping between the elastic and ER layers. Besides, the transverse displacements, *w*, of all points on any cross-section of the sandwich annular plate are constant.
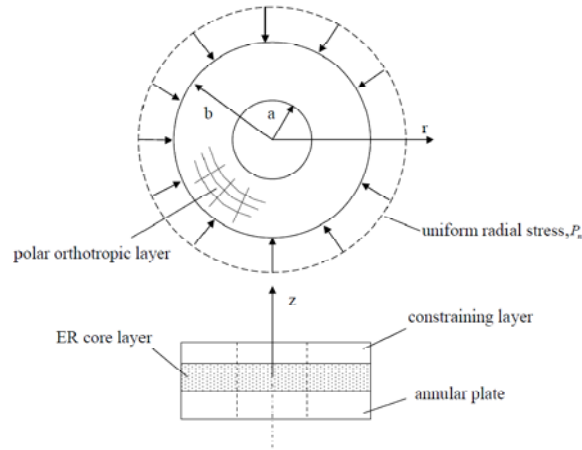

Fig. 1 Axisymmetric polar orthotropic sandwich annular plate with ER layer and constraining layer treatment and subjected to the uniform radial stress
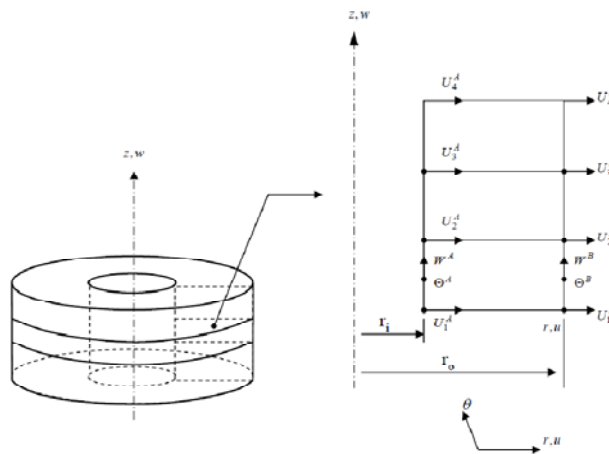

Fig. 2 The discrete layer annular finite element for three-layer element

In Fig. 2, the discrete layer annular finite element is utilized to formulate the problems of sandwich plate system. As shown in Fig. 1, the strain-displacement relation of the elastic layer can be expressed in terms of the in-plane displacements of the adjacent layer interfaces and the transverse displacement by considering the geometry of the sandwich annular plate system

$$d_i = \begin{Bmatrix} u_i(r,z,t) \\ w_i(r,z,t) \end{Bmatrix} = H_{1,i}(z) \begin{Bmatrix} U_i(r,t) \\ U_{i+1}(r,t) \\ W(r,t) \end{Bmatrix} \tag{1}$$

where $H_{1,i}(z) = \begin{bmatrix} (\frac{1}{2} - \frac{z}{h_i}) & (\frac{1}{2} + \frac{z}{h_i}) & 0 \\ 0 & 0 & 1 \end{bmatrix}$ is the transverse thickness interpolation matrix for

ith layer, u_i is the displacement for ith layer and w_i is the transverse displacement for ith layer, respectively. Then, the displacements of the interfaces for two-layer can be expressed in terms of the nodal degrees of freedom as following equation by using the interpolation in r-direction and the circumferential wave number m

$$\begin{Bmatrix} U_i(r,t) \\ U_{i+1}(r,t) \\ W(r,t) \end{Bmatrix} = H_2(r) q_i^e(t) \tag{2}$$

in which, $q_i^e = \left\{ U_i^A \quad V_i^A \quad U_{i+1}^A \quad V_{i+1}^A \quad W^A \quad \Theta^A \quad U_i^B \quad V_i^B \quad U_{i+1}^B \quad V_{i+1}^B \quad W^B \quad \Theta^B \right\}^{\mathrm{T}}$ is the vector of the nodal displacements of the element and $H_2(r)$ is the interpolation matrix.

Then, the strain-displacement relation for the ith layer of the system can be expressed as the following equation

$$\varepsilon_i = \begin{Bmatrix} \varepsilon_{r,i} \\ \varepsilon_{\theta,i} \\ \gamma_{rz,i} \end{Bmatrix} = D \, d_i \tag{3}$$

where ε_i is the strain vector and D is the differential operator matrix.

And, the stress-strain relation can be obtained and can be shown as follows

$$\sigma_i = C_i \varepsilon_i \tag{4}$$

in which, $\sigma_i = \left\{ \sigma_{r,i} \quad \sigma_{\theta,i} \quad \tau_{r\theta,i} \right\}^{\mathrm{T}}$, C_i is the elasticity matrix. Afterwards, the strain and kinetic energies of the element for ith layer can be expressed as the following forms

$$V_i^e = \frac{1}{2} \int_V \sigma_i^{\mathrm{T}} \, \varepsilon_i \, dV + \int_V \bar{\sigma}_i^{\mathrm{T}} \, \bar{\varepsilon}_i \, dV \tag{5}$$

$$T_i^e = \frac{1}{2} \int_V \rho_i \dot{u}_i^T \dot{u}_i dV \tag{6}$$

in which, $\overline{\sigma}_i$, $\overline{\varepsilon}_i$, and ρ_i are external load stress vector, non-linear strain vector, and the mass density of the *i*th layer, respectively and listed in detail in Appendix. Besides, the second term in Eq. (5) is additional strain energy due to external in-plane loads.

Then, the Hamilton's principle is used to derive element dynamic equilibrium equation and the following element differential equation can be express as follows by substituting Eqs. (1)-(4) into Eqs. (5) and (6)

$$M_i^e \ddot{U}_i^e + (K_i^e + G_i^e)U_i^e = 0 \tag{7}$$

where M_i^e, K_i^e, and G_i^e are element mass matrix, element stiffness matrix, and element geometric stiffness matrix due to the external in-plane load, respectively.

The following relations must be obtained first in order to combine the elemental matrices into the global stiffness and mass matrices

$$U_i^e = Tr_i^e U \tag{8}$$

where U and Tr_i^e are the global nodal co-ordinate vector and transformation matrix, respectively. Then, the equation of motion for the sandwich system can be express as follows by assembling the contribution of all elements of the system

$$M\ddot{U} + (K + G)U = 0 \tag{9}$$

where M, K, G are global mass, global stiffness, and global geometric stiffness matrix due to the external in-plane load, respectively and are given by

$$M = \sum_{i=1}^{3} (\sum_{e=1}^{N_i} Tr_i^{e^T} M_i^e Tr_i^e) \tag{10}$$

$$K = \sum_{i=1}^{3} (\sum_{e=1}^{N_i} Tr_i^{e^T} K_i^e Tr_i^e) \tag{11}$$

$$G = \sum_{i=1}^{3} (\sum_{e=1}^{N_i} Tr_i^{e^T} G_i^e Tr_i^e) \tag{12}$$

where N_i is the element number of the *i*th layer.

After that, the external load stress, $P(t)$, is assumed to be a periodic radial stress and presented as follows

$$P(t) = P_0 + P_t \cos\Theta t \tag{13}$$

where P_0, P_t, and Θ are static load factor, dynamic load factor, and the disturbance frequency, respectively. Additionally, the geometric stiffness matrix can be rewritten as the following form

$$G = G_0 + G_t \cos \Theta t \tag{14}$$

in which, G_0 is the static geometric stiffness matrix and G_t is dynamic geometric stiffness matrix. Then, the equation can be expressed as the following form called Mathieu-Hill equation

$$M\ddot{U} + (K + G_0 + G_t \cos \Theta t)U = 0 \tag{15}$$

In this study, the boundary of the dynamic instability can be calculated and obtained by using Bolotin's method (Bolotin 1964). The boundary of the dynamic instability of the sandwich system is formed according to the periodic solutions of the T $(2\pi / \Theta)$ and $2T$ $(4\pi / \Theta)$. The boundary of the primary instability region with period $2T$ is of practical important in mechanical applications and the solution can be expressed as follows

$$U(t) = \left[\{a_1\} \sin \frac{\Theta t}{2} + \{b_1\} \cos \frac{\Theta t}{2} \right] \tag{16}$$

and period solution with a period T in the form

$$U(t) = \left[\{a_2\} \sin(\Theta t) + \{b_2\} \cos(\Theta t) \right] \tag{17}$$

where $\{a_1\}$, $\{a_2\}$, $\{b_1\}$ and $\{b_2\}$ are undetermined constants.

Then, substituting Eqs. (16), (17) into Eq. (15) and rewriting the equations, the following non-trivial solution of the sandwich annular plate system can be obtained as the follows
for the solutions with a period *2T*

$$\begin{vmatrix} K^r + G_0^r - \dfrac{G_t^r}{2} - \dfrac{\Theta^2}{4} M & -K^j - G_0^j - \dfrac{G_t^j}{2} \\ K^j + G_0^j - \dfrac{G_t^j}{2} & K^r + G_0^r + \dfrac{G_t^r}{2} - \dfrac{\Theta^2}{4} M \end{vmatrix} = 0 \tag{18}$$

for the solutions with a period *T*

$$\begin{vmatrix} K^r + G_0^r & 0 & \dfrac{1}{2} G_t^r \\ -G_t^j & K^r + G_0^r - \Theta^2 M & -K^j - G_0^j \\ G_t^r & K^j + G_0^j & K^r + G_0^r - \Theta^2 M \end{vmatrix} = 0 \tag{19}$$

where the superscripts r and j denote the real and imaginary part of the matrices, respectively. Eqs. (18) and (19) are the equations of the boundary frequencies for the sandwich annular plate system. Then, the primary and secondary stability-instability boundaries of the polar orthotropic sandwich annular plate system with ER core treatment can be calculated and obtained by solving the complex equations.

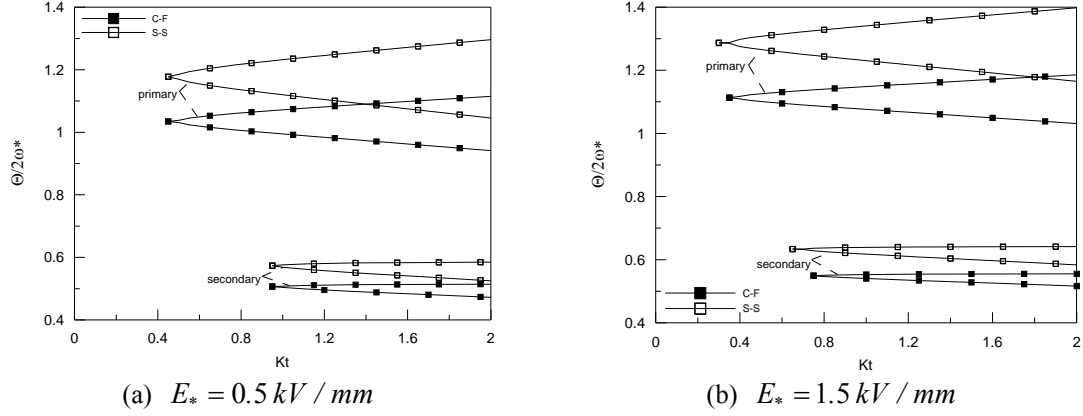(a) $E_* = 0.5\, kV\,/\,mm$ (b) $E_* = 1.5\, kV\,/\,mm$

Fig. 3 The primary and secondary instability regions of the polar orthotropic sandwich annular plate system with ER core layer. ($\tilde{a} = 0.1$, $\tilde{h}_1 = 0.2$, $\tilde{h}_2 = 0.5$, $\tilde{E}_1 = 1$, $\tilde{E}_3 = 1.5$, $K_o = 1$)

3. Results and discussions

The dynamic instability analysis of the sandwich annular plate with ER fluid core and constraining layer are presented in this study. And, the following non-dimensional parameters and some geometrical parameters are introduced for convenience:

$$b = 0.15\, m \ , \quad \tilde{a} = \frac{a}{b} \ , \quad \tilde{h}_2 = h_2/h_3 \ , \quad \tilde{h}_1 = h_1/h_3 \ , \quad \tilde{E}_1 = E_{\theta,1}/E_{r,1} \ , \quad \tilde{E}_3 = E_{\theta,3}/E_{r,3} \ , \quad \upsilon_{\theta r,i} = 0.29$$

(for i=1,3), $\upsilon_{r\theta,i} = E_{r,i}\upsilon_{\theta r}/E_{\theta,i}$ (for i=1,3), $\upsilon_2 = 0.49$, $h_3 = 0.5\, mm$, $\rho_1 = \rho_3 = 2700\, kg\,/\,m^3$, $\rho_2 = 1700\, kg\,/\,m^3$, $E_{r,1} = E_{r,3} = 70\, GPa$, $\kappa^2 = \pi^2/12$ (for i=1,3), $\kappa = 1$ (for i=2),

$D_k = \dfrac{E_3 h_3^2}{12(1-\upsilon_3^2)}$, $K_o = \dfrac{-P_0 h_3 b^2}{D_k}$, $K_t = \dfrac{-P_t h_3 b^2}{D_k}$. Additionally, $\omega*$ is the natural frequency

of the sandwich annular plate with the parameters $\tilde{a} = 0.1$, $\tilde{h}_1 = 0.1$, $\tilde{h}_2 = 0.5$, $h_3 = 0.5\, mm$, $K_o = K_t = 0$, and subjected to electric filed $E_* = 0.5\, kV\,/\,mm$ in the following discussions of the figures. On the other hand, damping effects of the sandwich system are provided by the ER fluid and only the electric field dependence of ER fluid needed to consider based on the existing model of ER material. Therefore, the complex modulus of ER fluid can be simplified into the following equation, which was experimentally measured by Don (1993)

$$G_2(E_*) = G' + jG'' \tag{17}$$

where E_* is the applied electric field strength in *kV/mm*, G' is the shear storage modulus ($G' \approx 15000E_*^2$), G'' is the loss modulus ($G'' \approx 6900$) and $j = \sqrt{-1}$, respectively.

The numerical results are compared with those results in order to validate present algorithm and calculations obtained in this study. Tables 1 and 2 show the numerical results compared with the results of polar orthotropic laminated annular plates (Lin and Tseng 1998) and full coverage sandwich annular plate (Roy and Ganesan 1993). It can be seen that numerical solutions solved by

present model are shown to have a good agreement and accuracy from the tables.

The effect of dynamic in-plane load K_t on primary and secondary instability regions of polar orthotropic annular plate system for C-F and S-S boundary conditions can be observed and shown in Figs. 3 (a) and 3(b), respectively. And, it can be seen that the tendency of the plate system are similar for different applying electric field strength according to the results. The primary and secondary instability regions of the polar orthotropic sandwich annular plate system with various applying electric field strength (E_*=0.5, 0.8, 1.5 *kV/mm*) are plotted in Fig. 4. Figs. 4(a) and 4(b) show the numerical results for C-f and S-S boundary conditions, respectively. The instability regions for polar orthotropic sandwich plate system will move to the higher disturbance frequency and smaller dynamic in-plane load. According to the characteristics of the ER fluid, the larger applying electric field strength will increase the stiffness of the sandwich plate system and it also can be seen that the tendency is similar for different boundary conditions.

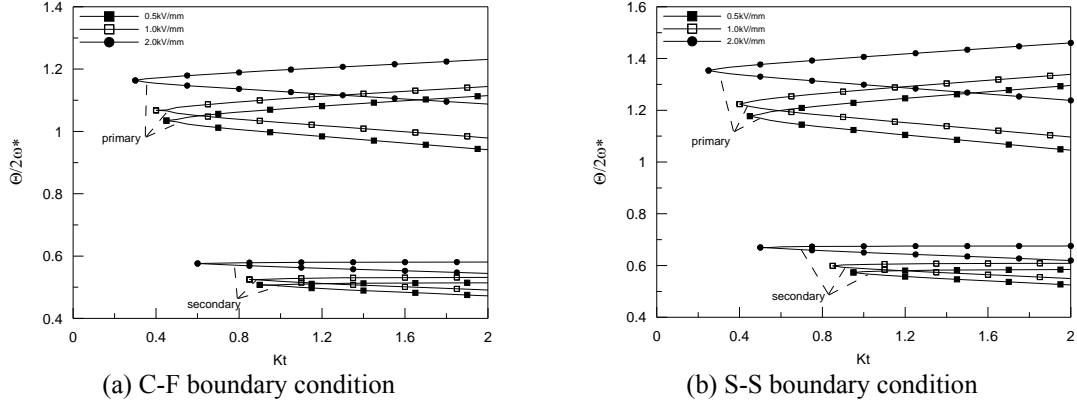(a) C-F boundary condition   (b) S-S boundary condition

Fig. 4 The primary and secondary instability regions of the polar orthotropic sandwich annular plate system with various applying electric field strength ($\widetilde{a} = 0.1$, $\widetilde{h}_1 = 0.2$, $\widetilde{h}_2 = 0.5$, $\widetilde{E}_1 = 1$, $\widetilde{E}_3 = 1.5$, $K_o = 1$)

Fig. 5 is the primary and secondary instability regions of the polar orthotropic sandwich annular plate system with various $\widetilde{E}_3$ (0.5, 0.8, 1.5). The primary and secondary instability regions of the sandwich plate system will shift to higher disturbance frequency as the parameter $\widetilde{E}_3$ increases.   It is because that the stiffness of the sandwich plate system will be larger with the increasing of $\widetilde{E}_3$. The plots of the primary and secondary instability regions for polar orthotropic sandwich annular plate system with various thickness of ER core layer are presented in Figs. 6 (a) and 6(b), respectively. The primary and secondary instability regions of the sandwich plate system will move downward and backward when the thickness of ER core layer increases. Additionally, the characteristics of the sandwich system are similar for C-F and S-S boundary conditions. Because of the system damping effects are provided by the ER fluid layer, so the stiffness of the system will decrease while the thickness of the ER core layer increasing.

Figs. 7 (a) and 7(b) show the effect of static in-plane load K_0 on primary and secondary instability regions of polar orthotropic annular plate system for C-F and S-S boundary conditions,

respectively. It can be observed that the primary and secondary instability regions will move downward as the static in-plane load increases and the variations of the sandwich plate system are similar for various boundary conditions. The effect of static in-plane load K_0 on primary and secondary instability regions for the polar orthotropic sandwich annular plate system with various applying electric field strength is plotted in Figs. 8 (a) and 8(b). Based on the numerical results, the primary and secondary instability regions of the sandwich plate system move smaller disturbance frequency with the increasing of static in-plane load K_0. Thus, the applying electric field strength can be utilized to control the dynamic behaviors of the sandwich plate system with ER fluid layer according to the numerical results.
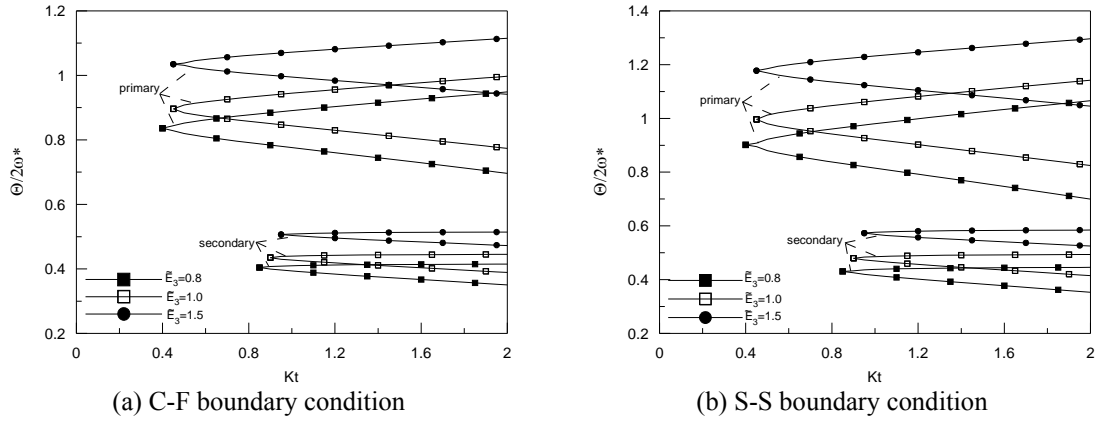
(a) C-F boundary condition	(b) S-S boundary condition

Fig. 5 The primary and secondary instability regions of the polar orthotropic sandwich annular plate system with various $\widetilde{E}_3$ ($\widetilde{a} = 0.1$, $\widetilde{h}_1 = 0.2$, $\widetilde{h}_2 = 0.5$, $\widetilde{E}_1 = 1$, $E_* = 0.5 kV/mm$, $K_o = 1$)

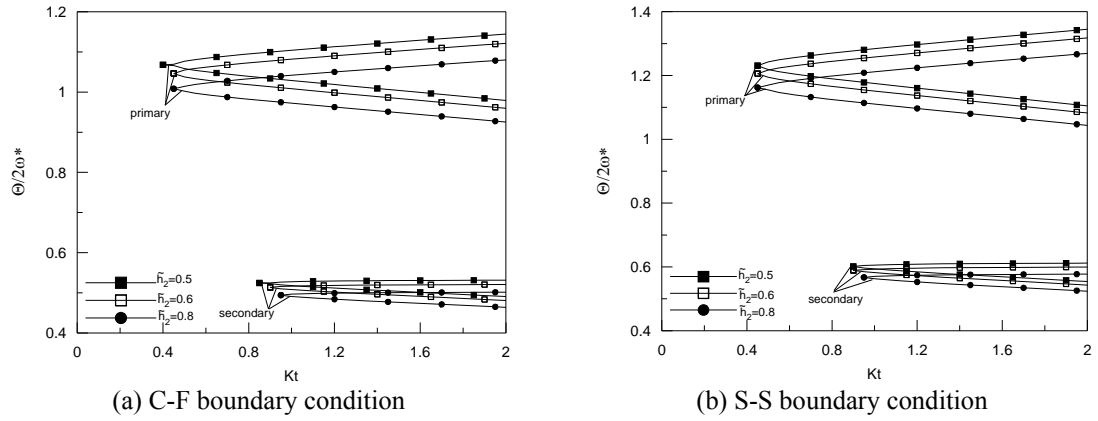|	
(a) C-F boundary condition	(b) S-S boundary condition

Fig. 6 The primary and secondary instability regions of the polar orthotropic sandwich annular plate system with various ER core layer thickness ($\widetilde{a} = 0.1$, $\widetilde{h}_1 = 0.2$, $\widetilde{E}_1 = 1$, $\widetilde{E}_3 = 1.5$, $E_* = 0.5 kV/mm$, $K_o = 1$)

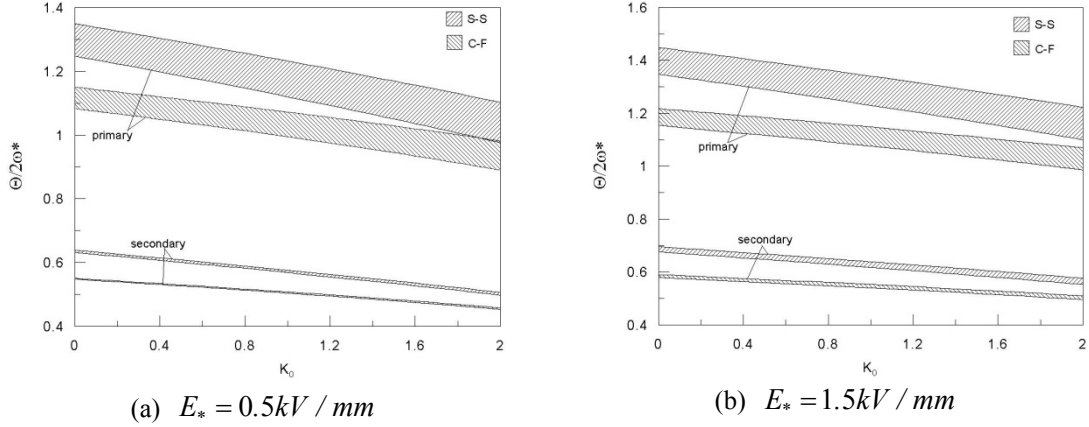(a) $E_* = 0.5 kV / mm$ (b) $E_* = 1.5 kV / mm$

Fig. 7 The primary and secondary instability regions of the polar orthotropic sandwich annular plate system with C-F and S-S boundary conditions ($\tilde{a} = 0.1$, $\tilde{h}_1 = 0.2$, $\tilde{h}_2 = 0.5$, $\tilde{E}_1 = 1$, $\tilde{E}_3 = 1.5$, $K_t = 1$)

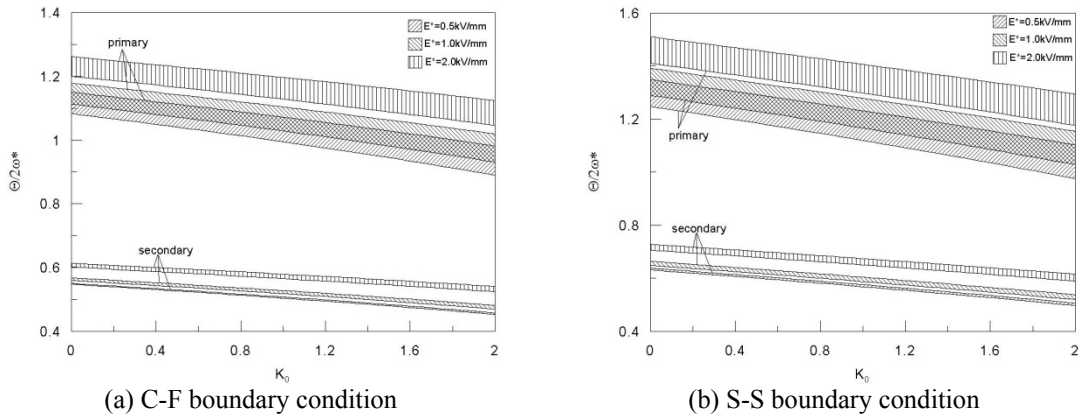(a) C-F boundary condition   (b) S-S boundary condition

Fig. 8 The primary and secondary instability regions of the polar orthotropic sandwich annular plate system with various applying electric field strength ($\tilde{a} = 0.1$, $\tilde{h}_1 = 0.2$, $\tilde{h}_2 = 0.5$, $\tilde{E}_1 = 1$, $\tilde{E}_3 = 1.5$, $K_t = 1$)

The effect of static in-plane load on primary and secondary instability regions for the polar orthotropic sandwich annular plate system with various $\tilde{E}_3$ (0.5, 0.8, 1.5) can be obtained in Figs. 9 (a) and 9(b). The primary and secondary instability regions of the polar orthotropic sandwich plate system will move upward to higher disturbance frequency and the width of the instability regions of the system will get smaller with the increasing of $\tilde{E}_3$. Additionally, the variations of the system are the same for C-F and S-S boundary conditions. Fig. 10 shows the effect of static in-plane load on primary and secondary instability regions for the polar orthotropic sandwich annular plate system with various ER core layer thicknesses. According to the numerical results,

the instability regions of the sandwich plate system move downward when the thickness of ER fluid layer is getting larger. It is because that the stiffness of the sandwich plate system will decrease as the thickness of ER fluid layer increases. The results for primary and secondary instability regions and different boundary conditions can be observed clearly in Figs. 10(a) and 10(b), respectively.
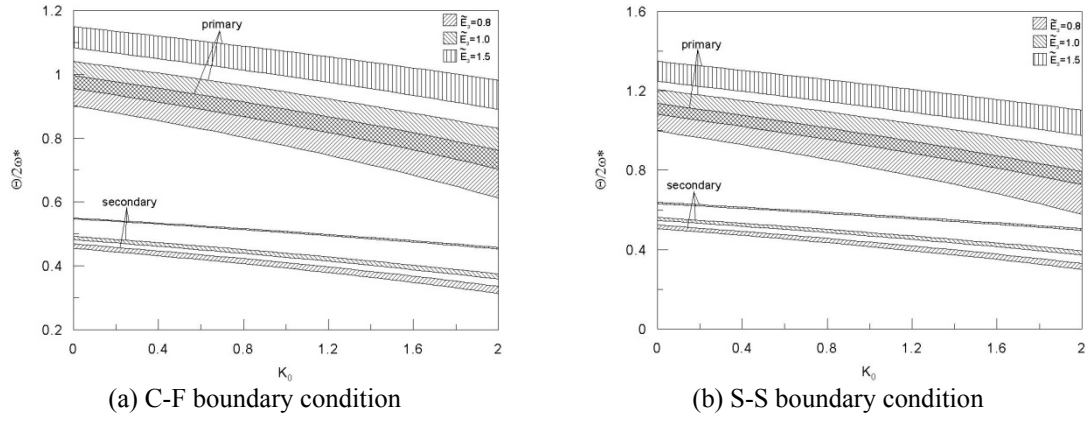

(a) C-F boundary condition   (b) S-S boundary condition

Fig. 9 The primary and secondary instability regions of the polar orthotropic sandwich annular plate system with various $\widetilde{E}_3$ ($\widetilde{a}=0.1$, $\widetilde{h}_1=0.2$, $\widetilde{h}_2=0.5$, $\widetilde{E}_1=1$, $E_*=0.5kV/mm$, $K_t=1$)

(a) C-F boundary condition   (b) S-S boundary condition
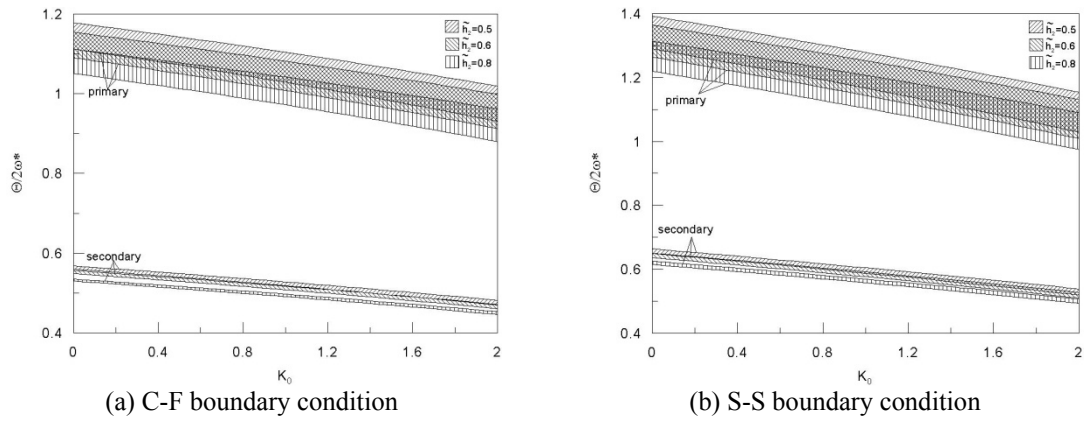
Fig. 10 The primary and secondary instability regions of the polar orthotropic sandwich annular plate system with various ER core layer thickness ($\widetilde{a}=0.1$, $\widetilde{h}_1=0.2$, $\widetilde{E}_1=1$, $\widetilde{E}_3=1.5$, $E_*=0.5kV/mm$, $K_t=1$)

4. Conclusions

In this paper, the axisymmetric dynamic instability of polar orthotropic sandwich annular plate with an ER fluid core layer studied. The boundaries of the stability-instability regions of the

sandwich annular plate are calculated and obtained by using the discrete layer annular finite element method and the harmonic balance method. And, a complex description of the viscoelastic material is adopted for the ER fluid in this investigation. Thus, the controllable devices, such as some mechanical or micro-mechanical devices, can be designed and acted as novel controlled devices according to present numerical results.

Numerical results are shown that the applying electric field strength will change the stiffness of polar orthotropic sandwich plate system and the instability regions of the sandwich plate system can be changed and controlled by applying different electric field strength. Besides, the stiffness of the sandwich plate system can increase while increasing of $\widetilde{E}_3$. It also can be utilized to change the dynamic behaviors of the sandwich plate system. As to the thickness of ER fluid layer, the instability regions of the sandwich annular plate system will be changed and controlled with various thickness of the ER layer. Thus, the applying electric field strength, the ER fluid layer, and the parameter $\widetilde{E}_3$ are shown to have significant effects on the instability regions of the sandwich plate system and can be utilized to control and change the dynamic behaviors of polar orthotropic sandwich plate system.

Finally, the present results hope to provide the basic information for practical applications and can be utilized to design some active controllable and more stable mechanical devices

References

Bolotin, V.V. (1964), *The dynamic stability of elastic system*, Holden-Day San Francisco.

Chen, L.W. and Hwang, J.R. (1988), "Axisymmetric dynamic stability of transverse isotropic Mindlin circular plates", *J. Sound Vib.*, **121**(2), 307-315.

Chen, Y.R. and Chen, L.W. (2004), "Axisymmetric parametric resonance of polar orthotropic sandwich annular plates", *Compos. Struct.*, **65**(3-4), 269-277.

Don, D.L. (1993), *An investigation of electrorheological material adoptive structures*, Master's Thesis Lehigh University, Bethlehem, Pennsylvania.

Don, D.L. and Coulter, J.P. (1995), "An analytical and experimental investigation of electrorheological material based adaptive beam structures", *J. Intel. Mat. Syst. Str.*, **6**(6), 846-853.

Dumir, P.C. and Shingal L. (1985), "Axisymmetric postbuckling of orthotropic thick annular plates", *Acta Mech.*, **56**(3-4), 229-242.

Ilyasov, M.H. and Akoz, A.Y. (2000), "The vibration and dynamic stability of viscoelastic plates", *Int. J. Eng. Sci.*, **38**(6), 695-714.

Kang, Y.K., Kim, J. and Choi, S.B. (2001), "Passive and active damping characteristics of smart electro-rheological composite beams", *Smart Mater. Struct.*, **10**(4), 724-729.

Lee, C.Y. (1992), "Dynamic characteristics of a smart beam featuring embedded electro-rheological fluids", *Proceedings of the 9th Nat Conf on Mech. Eng. CSME*.

Lin, C.C. and Tseng, C.S. (1998), "Free vibration of polar orthotropic laminated circular and annular plates", *J. Sound Vib.*, **209**(5), 797-810.

Oyadiji, S.O. (1996), "Application of electro-rheological fluids for constrained layer damping treatment of structures", *J. Intel. Mat. Syst. Str.*, **7**(5), 541-549.

Phani, A.S. and Venkatraman, K. (2003), "Vibration control of sandwich beams using electro-rheological fluids", *Mech. Syst. Signal Pr.*, **17**(5), 1083-1095.

Pawlus, D. (2011), "Solution to the problem of axisymmetric and asymmetric dynamic instability of three-layered annular plates", *Thin Wall. Struct.*, **49**(5), 660-668.

Ramachandra, L.S. and Panda, S.K. (2012), "Dynamic instability of composite plates subjected to non-uniform in-plane loads", *J. Sound Vib.*, **331**, 53-65.

Roy, P.K. and Ganesan, N. (1993), "A vibration and damping analysis of circular plates with constrained damping layer treatment", *Comput. Struct.*, **49**, 269-274.

Wang, X., Wang, X. and Shi, X. (2006), "Accurate buckling loads of thin rectangular plates under parabolic edge compressions by the differential quadrature method", *Int. J. Mech. Sci.*, **49**(4), 447-453.

Yalcintas. M. and Coulter, J.P. (1995), "Analytical modeling of electrorheological material based adaptive beams", *J. Intel. Mat. Syst. Str.*, **6**(4), 488-497.

Yeh, J.Y. (2007), "Vibration control of a sandwich annular plate with an electrorheological fluid core layer", *Smart Mater. Struct.*, **16**(3), 837-842.

Yeh, J.Y., Chen, J.Y., Lin, C.T. and Liu, C.Y. (2009), "Damping and vibration analysis of polar orthotropic annular plates with ER treatment", *J. Sound Vib.*, **325**(1-2), 1-13.

Yeh, J.Y. (2011), "Parametric resonance of axisymmetric sandwich annular plate with ER core layer and constraining layer", *Smart Struct. Syst.*, **8**(5), 487-499.

Zhong, H. and Gu, C. (2006), "Buckling of simply supported rectangular Reissner-Mindlin plates subjected to linearly varying in plane loading", *J. Eng. Mech.- ASCE*, **132**(5), 578-581.

Zhou, Y.F. and Wang, Z.M. (2009), "Dynamic behaviors of axially moving viscoelastic plate with varying thickness", *J. Sound Vib.*, **22**, 276-281.

CC

Appendix

1. $H_2(r) = \begin{bmatrix} \phi_u^A & 0 & 0 & 0 & \phi_u^B & 0 & 0 & 0 \\ 0 & \phi_u^A & 0 & 0 & 0 & \phi_u^B & 0 & 0 \\ 0 & 0 & \phi_w^A & \phi_\Theta^A & 0 & 0 & \phi_w^B & \phi_\Theta^B \end{bmatrix}$, where $\phi_u^A = (1-\xi)$, $\phi_u^B = \xi$,

$\phi_w^A = (1 - 3\xi^2 + 2\xi^3)$, $\phi_w^B = (3\xi^2 - 2\xi^3)$, $\phi_\Theta^A = (\xi - 2\xi^2 + \xi^3)$, $\phi_\Theta^B = (-\xi^2 + \xi^3)$,

$\xi = \dfrac{r - r_i}{r_0 - r_i}$.

2. $D = \begin{bmatrix} \dfrac{\partial}{\partial r} & 0 \\ \dfrac{1}{r} & 0 \\ \dfrac{\partial}{\partial z} & \dfrac{\partial}{\partial r} \end{bmatrix}$.

3. $C_i = \begin{bmatrix} C_{11,i} & C_{12,i} & 0 \\ C_{21,i} & C_{22,i} & 0 \\ 0 & 0 & C_{44,i} \end{bmatrix}$,

for isotropic ER material, $C_{11,2} = C_{22,2} = \dfrac{E_2}{1 - \upsilon_2^2}$, $C_{12,2} = C_{21,2} = \dfrac{\upsilon_2 E_2}{1 - \upsilon_2^2}$, $C_{44,2} = \dfrac{E_2}{2(1 + \upsilon_2)}$, $\upsilon_2 = 0.499$, respectively.

For polar orthotropic material $(i=1,3)$, $C_{11,i} = \dfrac{E_{r,i}}{1 - \upsilon_{r\theta,i}\upsilon_{\theta r,i}}$, $C_{22,i} = \dfrac{E_{\theta,i}}{1 - \upsilon_{r\theta,i}\upsilon_{\theta r,i}}$,

$C_{12,i} = C_{21,i} = \dfrac{\upsilon_{\theta r,i} E_{r,i}}{1 - \upsilon_{r\theta,i}\upsilon_{\theta r,i}}$, $C_{44,i} = \kappa G_{rz,i}$, respectively. In the above equations, E_i is the Young's modulus, υ_i is the Poisson ration, and κ is the shear correction factor.

4. $\bar{\sigma}_i = \begin{Bmatrix} \bar{\sigma}_{r,i} \\ \bar{\sigma}_{\theta,i} \\ \bar{\tau}_{rz,i} \end{Bmatrix} = C_i D(H_{1,i} H_2)\overline{U}_i^e$, $\bar{\varepsilon}_i = \begin{Bmatrix} \dfrac{1}{2}(\dfrac{\partial u_i}{\partial r})^2 + \dfrac{1}{2}(\dfrac{\partial w_i}{\partial r})^2 \\ \dfrac{1}{2}(\dfrac{u_i}{r})^2 \\ \dfrac{\partial u_i}{\partial r}\dfrac{\partial u_i}{\partial z} \end{Bmatrix}$,

where $\overline{U}_i^e$ is the equilibrium nodal displacement vector of annular element for *i*th layer.

5. $M_i^e = \displaystyle\int_V (DH_{1,i}H_2)^{\mathrm{T}} C_i^{\mathrm{T}} (DH_{1,i}H_2)dV$, $K_i^e = \displaystyle\int_V \rho_i (H_{1,i}H_2)^{\mathrm{T}} (H_{1,i}H_2)dV$,

$$G_i^e = 2\int_V [(D_1 H_4 H_{1,i} H_2)^T \hat{\sigma}_i^e (D_2 H_4 H_{1,i} H_2) + (D_1 H_5 H_{1,i} H_2)^T \hat{\sigma}_i^e (D_2 H_5 H_{1,i} H_2)$$

$$+ \frac{1}{2}(D_3 H_5 H_{1,i} H_2)^T \hat{\sigma}_i^e (D_3 H_5 H_{1,i} H_2)]dV ,$$

in which, $D_1 = \left\{\begin{array}{c} \frac{1}{2}\frac{\partial}{\partial r} \\ 0 \\ \frac{\partial}{\partial r} \end{array}\right\}$, $D_2 = \left\{\begin{array}{c} \frac{\partial}{\partial r} \\ 0 \\ \frac{\partial}{\partial z} \end{array}\right\}$, $D_3 = \left\{\begin{array}{c} 0 \\ \frac{1}{r} \\ 0 \end{array}\right\}$, $\hat{\sigma}_i^e = \begin{bmatrix} \overline{\sigma}_{r,i}^e & 0 & 0 \\ 0 & \overline{\sigma}_{\theta,i}^e & 0 \\ 0 & 0 & \overline{\tau}_{rz,i}^e \end{bmatrix}$,

$H_4 = \begin{bmatrix} 1 & 0 \end{bmatrix}$, $H_5 = \begin{bmatrix} 0 & 1 \end{bmatrix}$.

Table 1 Non-dimensional natural frequency of polar orthotropic laminated annular plates

		Non-dimensional natural frequency	
b/a	b/h	Present	Lin and Tseng (1998)
0.1	10	13.471	13.526
	20	14.042	13.936
	50	14.238	14.147
	100	14.267	14.178
0.5	10	20.818	20.636
	20	21.959	21.851
	50	22.318	22.233
	100	22.371	22.290

Table 2 Comparison between published and proposed methods for the full coverage annular plate

		Mode (n,m)				
		(0,0)	(0,1)	(0,2)	(0,3)	(0,4)
Natural frequency (Hz)	Roy and Ganesan (1993)	74.38	73.08	96.38	142.8	203.7
	Present	74.44	73.00	96.20	144.00	205.20
Modal loss Factor	Roy and Ganesan (1993)	0.1127	0.09576	0.1021	0.1212	0.1177
	Present	0.1128	0.09542	0.1016	0.1210	0.1170